

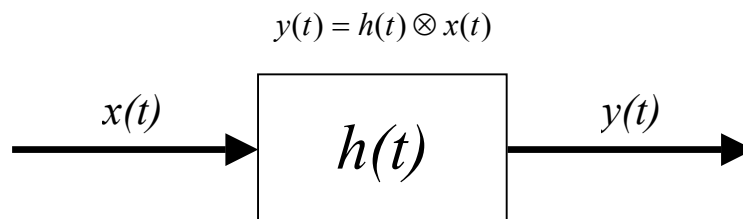
Glitch Simulation - SPIRE-UOL-NOT-002207, v0.1

Trevor Fulton
07/05/2004

The purpose of this work is to gain a greater understanding of the response of the overall SPIRE detector system. In particular, this effort will be geared toward generating a realistic simulation of the response of the SPIRE bolometers to a cosmic ray event.

Background

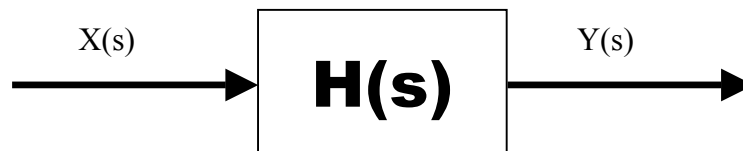
The response of the detector system is a function of the input to the system and the transfer function of the system itself. In the time domain, the input and output signals may be represented as $x(t)$ and $y(t)$ respectively. The relation between the input and the output signals is through the system transfer function, $h(t)$, and is given by



The system may also be characterized in the Laplace domain. Here the input and output signals, $\mathbf{X(s)}$ and $\mathbf{Y(s)}$ respectively, are simply the Laplace transforms of the time domain input and output signals. The equation that relates the system input and output signals in the Laplace domain is:

$$\mathbf{Y(s)} = \mathbf{H(s)}\mathbf{X(s)}$$

Where $\mathbf{H(s)}$ is the Laplace transform of the time domain system transfer function, $h(t)$.



SPIRE Detectors

The transfer functions for the SPIRE detector systems are given by the following¹:

SPECTROMETER, 6-POLE BESSEL LOW PASS FILTER

$$H_s(s) = 3.05 \times \frac{1}{1 + 7.58 \times 10^{-3} s + 16.03 \times 10^{-6} s^2} \\ \times \frac{1}{1 + 3.21 \times 10^{-3} s + 10.89 \times 10^{-6} s^2} \\ \times \frac{1}{1 + 6.26 \times 10^{-3} s + 14.65 \times 10^{-6} s^2}$$

PHOTOMETER, 4-POLE BESSEL LOW PASS FILTER

$$H_p(s) = 1.93 \times \frac{1}{1 + 42.58 \times 10^{-3} s + 503 \times 10^{-6} s^2} \times \frac{1}{1 + 24.96 \times 10^{-3} s + 400 \times 10^{-6} s^2}$$

In addition to the detector filters, the response of the detector system should be influenced by the thermal response of the bolometers themselves, **H_t(s)**. Based on data from the SPIRE bolometers², the thermal response of the bolometers can be approximated an RC low-pass filter with a time constant, τ_t , equal to 18ms. That is, **H_t(s)** may be written as:

$$H_t(s) = \frac{\omega_t}{s + \omega_t} \\ \omega_t = 55.5 \frac{\text{rad}}{\text{s}} = 1 / \tau_t = 1 / (18\text{ms})$$

As the detector system is affected by the both the thermal and electrical response of the detectors, the overall detector system transfer function, **H(s)** or $h(t)$, will be a combination of the two transfer functions. In the Laplace domain, the overall system transfer function is simply the product of the constituent transfer functions. In the case of the SPIRE detector systems, this results in:

<u>SPECTROMETER</u>	H(s) = H_t(s) H_s(s)
<u>PHOTOMETER</u>	H(s) = H_t(s) H_p(s)

The overall system transfer functions for the SPIRE detectors may therefore be expressed as follows:

¹ See Appendix 1

² See Appendix 2

SPECTROMETER

$$\begin{aligned} H(s) &= H_b(s)H_s(s) \\ &= 3.05 \times \left[\frac{\omega_t}{s + \omega_t} \right] \times \left[\frac{1}{1 + 7.58 \times 10^{-3}s + 16.03 \times 10^{-6}s^2} \right] \\ &\quad \times \left[\frac{1}{1 + 3.21 \times 10^{-3}s + 10.89 \times 10^{-6}s^2} \right] \times \left[\frac{1}{1 + 6.26 \times 10^{-3}s + 14.65 \times 10^{-6}s^2} \right] \\ &= \frac{A}{s + \omega_t} + \frac{B^*}{s + \alpha_1 + j\beta_1} + \frac{B}{s + \alpha_1 - j\beta_1} + \frac{C^*}{s + \alpha_2 + j\beta_2} + \frac{C}{s + \alpha_2 - j\beta_2} + \frac{D^*}{s + \alpha_3 + j\beta_3} + \frac{D}{s + \alpha_3 - j\beta_3} \end{aligned}$$

where:

- $A = 4.4475$, $\omega_t = 55.56$
- $B = 15.583$, $\angle B = 138.116$
- $\alpha_1 = 236.432$, $\beta_1 = 80.518$
- $C = 1.1109$, $\angle C = -120.205$
- $\alpha_2 = 147.382$, $\beta_2 = 264.775$
- $D = 9.937$, $\angle D = 0.5917$
- $\alpha_3 = 211.604$, $\beta_3 = 153.242$

PHOTOMETER

$$\begin{aligned} H(s) &= H_b(s)H_p(s) \\ &= 1.93 \times \left[\frac{\omega_t}{s + \omega_t} \right] \times \left[\frac{1}{1 + 42.58 \times 10^{-3}s + 503 \times 10^{-6}s^2} \times \frac{1}{1 + 24.96 \times 10^{-3}s + 400 \times 10^{-6}s^2} \right] \\ &= \frac{A}{s + \omega_t} + \frac{B^*}{s + \alpha_1 + j\beta_1} + \frac{B}{s + \alpha_1 - j\beta_1} + \frac{C^*}{s + \alpha_2 + j\beta_2} + \frac{C}{s + \alpha_2 - j\beta_2} \end{aligned}$$

where:

- $A = 28.458$, $\omega_t = 55.56$
- $B = 27.891$, $\angle B = -124.551^\circ$
- $\alpha_1 = 42.326$, $\beta_1 = 14.021$
- $C = 0.52675$, $\angle C = 67.722^\circ$
- $\alpha_2 = 4.190$, $\beta_2 = 39.071$

Response to a Cosmic Ray Event

As a first attempt to characterize the output of the detector system to a cosmic ray event, let us represent the cosmic ray event with a Dirac delta function, $x(t) = \delta(t)$. Since the Laplace transform of a Dirac delta function is equal to one, $\mathbf{Y(s)} = \mathbf{H(s)}\mathbf{X(s)} = \mathbf{H(s)}$, the response of the detector system is simply the system transfer function itself. Converting the system response from the Laplace domain to the time domain for the spectrometer and the photometer systems gives:

SPECTROMETER

$$\begin{aligned} y(t) = h(t) &= Ae^{-\omega_t t} + 2|(B)|e^{-\alpha_1 t} \cos(\beta_1 t + \angle B) \\ &\quad + 2|(C)|e^{-\alpha_2 t} \cos(\beta_2 t + \angle C) + 2|(D)|e^{-\alpha_3 t} \cos(\beta_3 t + \angle D) \end{aligned}$$

with:

- $A = 4.4475,$ $\omega_t = 55.56$
- $B = 15.583,$ $\angle B = 138.116^\circ$
- $\alpha_1 = 236.432,$ $\beta_1 = 80.518$
- $C = 1.1109,$ $\angle C = -120.205^\circ$
- $\alpha_2 = 147.382,$ $\beta_2 = 264.775$
- $D = 9.937,$ $\angle D = 0.5917^\circ$
- $\alpha_3 = 211.604,$ $\beta_3 = 153.242$

PHOTOMETER

$$y(t) = h(t) = Ae^{-\omega_t t} + 2|(B)|e^{-\alpha_1 t} \cos(\beta_1 t + \angle B) + 2|(C)|e^{-\alpha_2 t} \cos(\beta_2 t + \angle C)$$

with:

- $A = 28.458,$ $\omega_t = 55.56$
- $B = 27.891,$ $\angle B = -124.551^\circ$
- $\alpha_1 = 42.326,$ $\beta_1 = 14.021$
- $C = 0.52675,$ $\angle C = +67.722^\circ$
- $\alpha_2 = 4.190,$ $\beta_2 = 39.071$

The curves in the following figure are simulations of the output signal for the spectrometer (black) and photometer (red) systems in response to a simulated cosmic ray event.

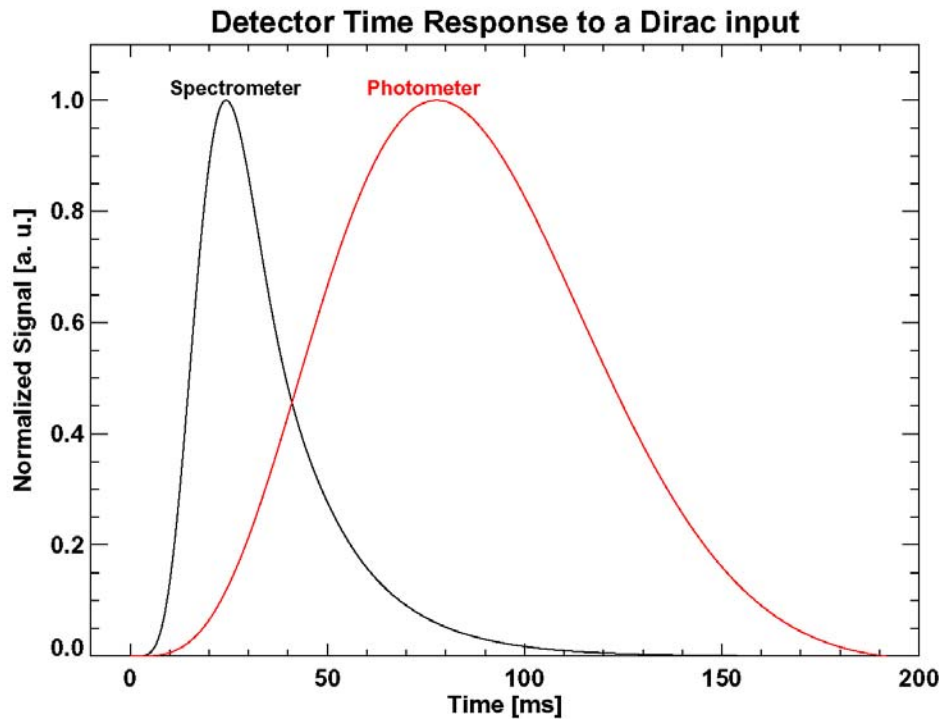


Figure 1 Time Response of SPIRE Detectors to a Simulated Cosmic Ray Event

Appendix 1 SPIRE Detector Systems

The spectrometer detector system and the photometer detector system each contain multi-pole low pass Bessel filters³. The circuit diagrams and transfer functions (spectrometer, $H_s(s)$: photometer, $H_p(s)$) for the spectrometer and photometer systems are shown below.

SPECTROMETER

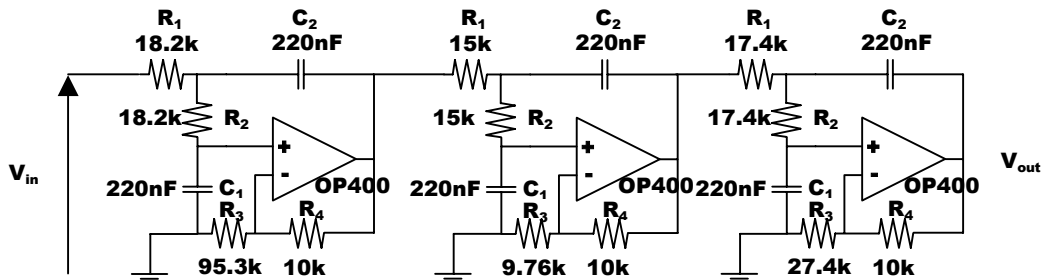


Figure A1.1 Spire Spectrometer Low Pass Filter Circuit⁴

$$H_s(f) = \frac{V_{out}}{V_{in}} = 3.05 \times \frac{1}{1 + 7.58p + 4p^2} \times \frac{1}{1 + 3.21p + 3.3p^2} \times \frac{1}{1 + 6.26p + 3.828p^2}$$

where: $p = j2\pi f$

PHOTOMETER

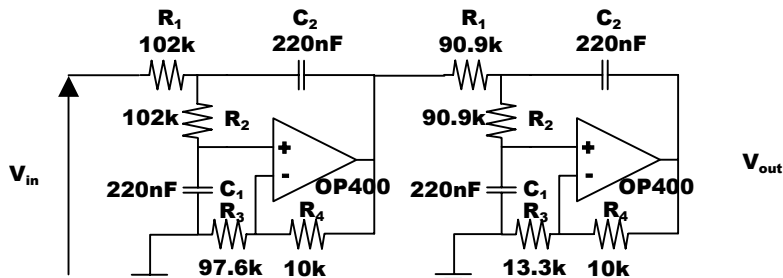


Figure A1.2 Spire Photometer Low Pass Filter Circuit⁵

³ SPIRE DCU Design Document, 18 February 2003

⁴ SPIRE DCU Design Document, 18 February 2003, p. 51

⁵ SPIRE DCU Design Document, 18 February 2003, p. 39

$$H_p(f) = \frac{V_{out}}{V_{in}} = 1.93 \times \frac{1}{1 + 42.58p + 503p^2} \times \frac{1}{1 + 24.96p + 400p^2}$$

where: $p = j2\pi f$

On closer inspection, the low-pass filter circuits listed in the SPIRE DCU Design Document each appear to follow the Sallen-Key architecture (see Figure A1.3).

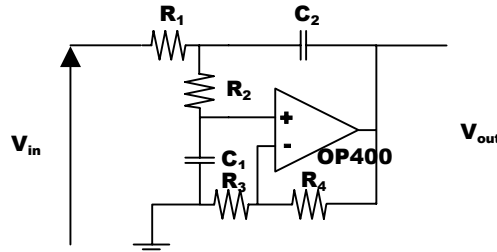


Figure A1.3 Low Pass Sallen-Key Architecture

The ideal transfer function for the Sallen-Key architecture is given by:

$$H(f) = \frac{\frac{R_3 + R_4}{R_3}}{1 + (R_1C_1 + R_2C_1 + R_1C_2(-\frac{R_4}{R_3}))p + (R_1R_2C_1C_2)p^2}$$

where: $p = j2\pi f$

Using the equation listed above and the component values as given in the SPIRE DCU Design Document, the transfer functions for the spectrometer and photometer low-pass filters are now given as:

SPECTROMETER

$$H_s(f) = 3.05 \times \frac{1}{1 + 7.58 \times 10^{-3} p + 16.03 \times 10^{-6} p^2}$$

$$\times \frac{1}{1 + 3.21 \times 10^{-3} p + 10.89 \times 10^{-6} p^2}$$

$$\times \frac{1}{1 + 6.26 \times 10^{-3} p + 14.65 \times 10^{-6} p^2}$$

PHOTOMETER

$$H_p(f) = 1.93 \times \frac{1}{1 + 42.58 \times 10^{-3} p + 503 \times 10^{-6} p^2} \times \frac{1}{1 + 24.96 \times 10^{-3} p + 400 \times 10^{-6} p^2}$$

The following figures show the frequency response of the photometer and spectrometer low-pass filters based on the modified transfer functions.

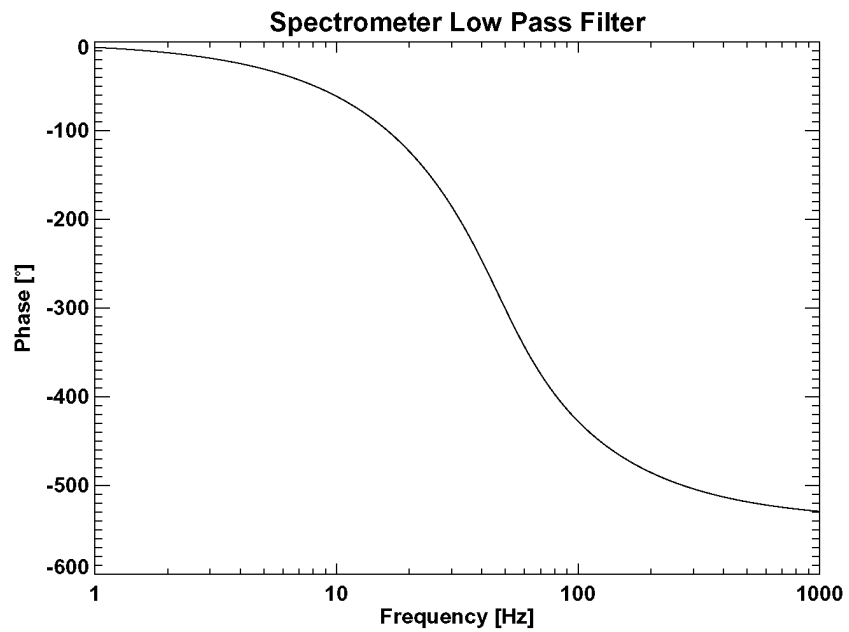
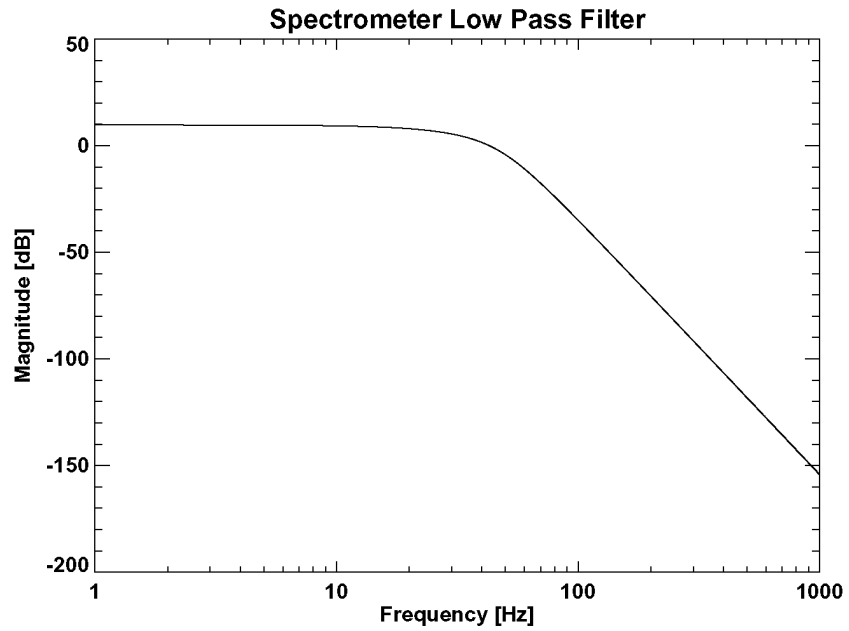


Figure A1.4 Spectrometer Low Pass Filter Frequency Response Using Modified Transfer Function

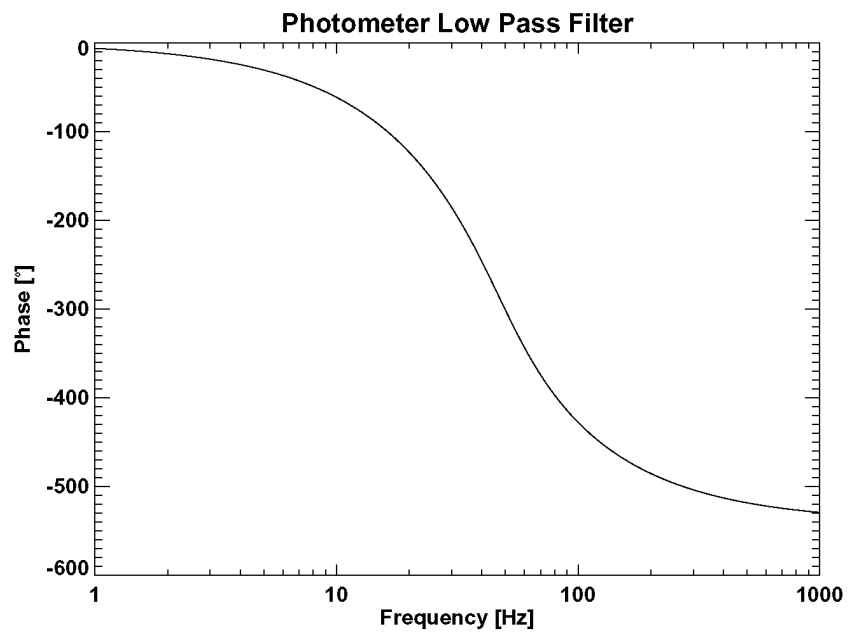
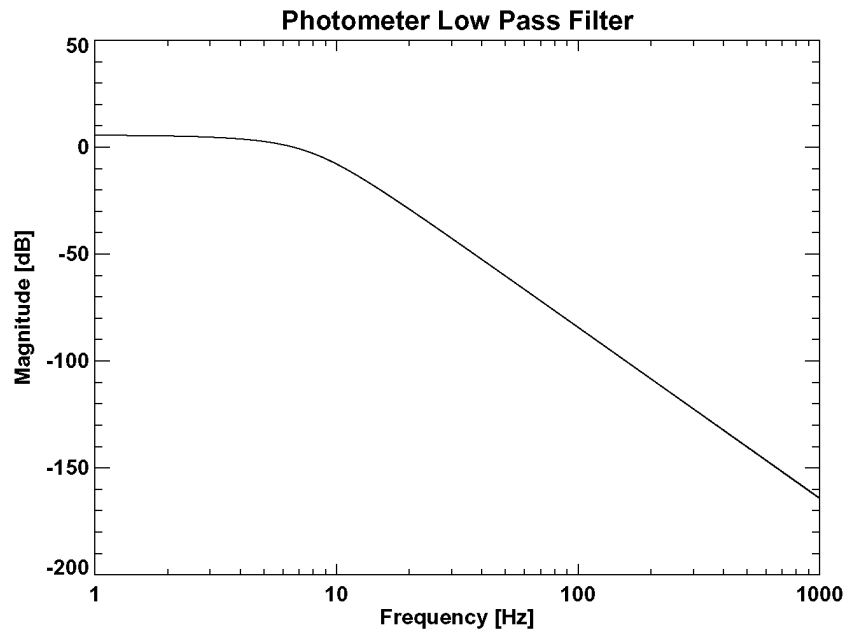


Figure A1.5 Photometer Low Pass Filter Frequency Response Using Modified Transfer Function

These curves displayed in Figures A1.4 and A1.5 show good agreement with those in the SPIRE DCU Design Document⁶. On this basis, the modified transfer functions derived above and not those listed in the SPIRE DCU Design Document will be taken as correct.

⁶ *SPIRE DCU Design Document*, 18 February 2003, pp. 52 (spectrometer), 40 (photometer)

Appendix 2: Bolometer Thermal Response

The thermal response of the SPIRE bolometers has been derived from data from the SPIRE CQM of 9-11 February 2004 and on work done by Bernhard Schulz from JPL. The plots in Figure A1 show the measured frequency response for two of the PLW bolometers. The fitted line represents the theoretical frequency response of a single-pole low-pass filter with the thermal time constant, $\tau = \text{Tau}$, as listed. From Figure A2.1 we can see that the data and theoretical curve agree fairly well.

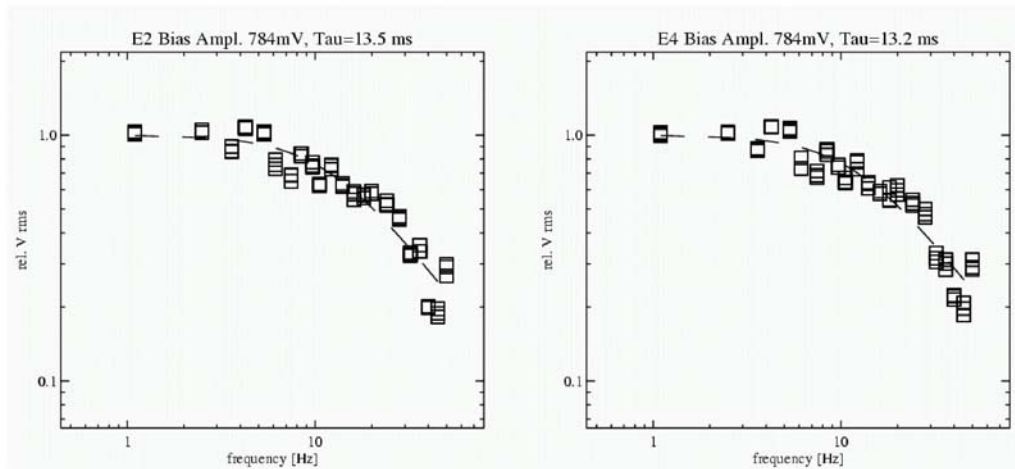


Figure A2.1 Measured Frequency Response of Selected SPIRE PLW Bolometers

The plot shown in Figure A2.2 is a histogram of the thermal time constants for all of the PLW bolometers. Based on this histogram, a value of 18ms was chosen as a representative value for the PLW bolometer thermal time constant.

SPIRE CQM Time Constants (38 Det.)

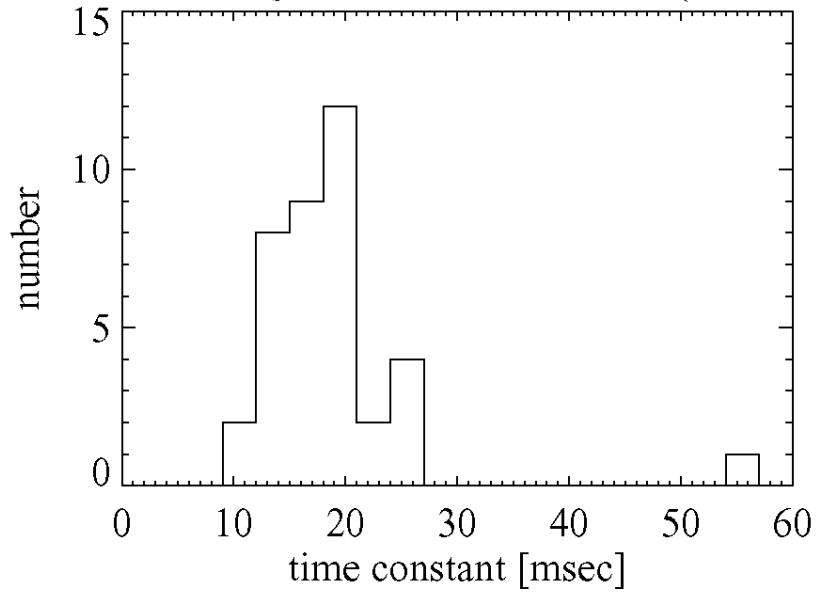


Figure A2.2 Measured Thermal Time Constants of SPIRE PLW Bolometers

Using the nominal value of 18ms for the thermal time constant of the bolometers, one can simulate their frequency response. The following figures show the simulated frequency response of the bolometers.

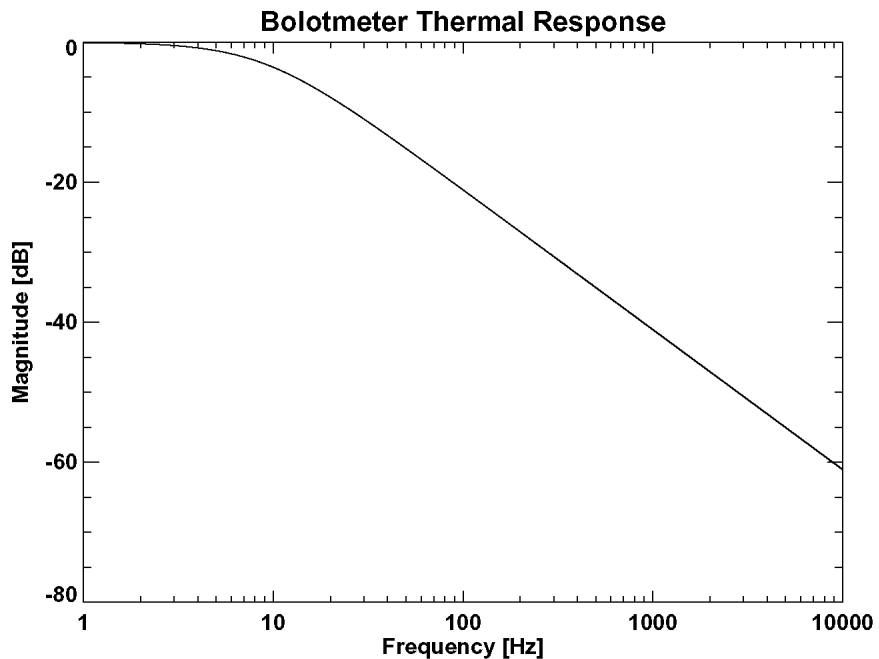


Figure A2.3 Simulated Frequency Response of SPIRE PLW Bolometers

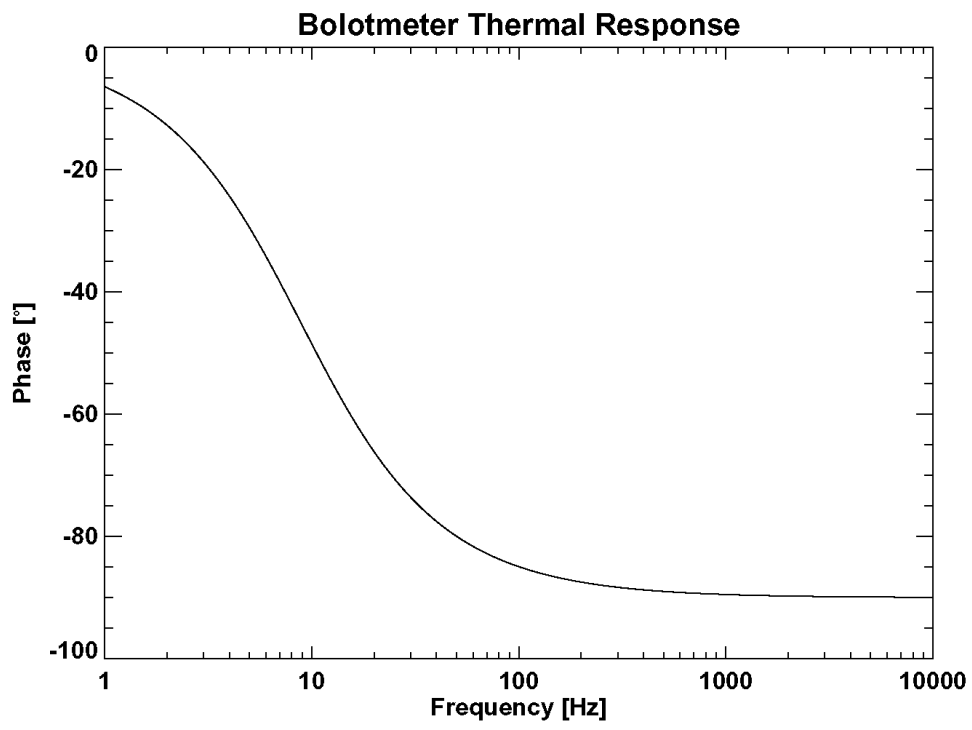


Figure A2.4 Simulated Frequency Response of SPIRE PLW Bolometers